Angular dependence and origin of asymmetric magnetization reversal in exchange-biased $Fe/FeF_2(110)$

A. Tillmanns,[1,*] S. Oertker,[1,†] B. Beschoten,[1] G. Güntherodt,[1,‡] J. Eisenmenger,[2,§] and I. K. Schuller[2]
[1]*Physikalisches Institut IIA, RWTH Aachen University, 52056 Aachen, Germany*
[2]*Department of Physics, University of California, San Diego, La Jolla, California 92093-0319, USA*
(Received 25 May 2008; published 3 July 2008)

Asymmetric magnetization reversal in exchange-biased Fe/FeF_2 has been analyzed by magneto-optic Kerr loops transverse to the measuring field. Noncollinear cooling-field and measuring-field directions yield a complex phase diagram of distinct transverse reversal modes. The phase diagram is simulated by a simple total-energy-density model, including noncollinear anisotropies and magnetization rotation. Asymmetric magnetization reversal occurs for 360° of cooling-field directions if these are noncollinear with measuring-field and exchange-bias directions except near easy and hard axes.

DOI: 10.1103/PhysRevB.78.012401 PACS number(s): 75.60.Jk, 75.30.Et, 75.50.Ee, 75.70.Cn

A bilayer system of an antiferromagnetic (AFM) and a ferromagnetic (FM) layer exhibits a shift of the hysteresis loop along the field axis, the so-called exchange bias (EB).[1–3] This shift may be observed after cooling the system below the Néel temperature of the AFM in an external magnetic field. Exchange-biased systems can, in addition to an enhanced coercivity, exhibit a very pronounced asymmetry of the hysteresis loops.[4]

The magnetization reversal asymmetry was first investigated by polarized neutron reflectometry (PNR) in Fe/FeF_2.[5] Different reversal mechanisms have been attributed to the left- and right-side coercive fields of the hysteresis loop as due to, respectively, coherent magnetization rotation and domain-wall nucleation as well as propagation. While the former mechanism was identified by a magnetization component transverse to the magnetic-field direction, the latter was assigned due to the absence of a transverse magnetization component. This behavior raises the general question as to the origin of this unprecedented asymmetry in any switchable hysteretic physical system. Moreover, the asymmetry in the hysteresis loop might also be reversed. For instance, in Co/CoO magnetization rotation has been found only on the right side of the hysteresis loop.[6]

A fast and powerful experimental probe of coherent magnetization rotation is the magneto-optic Kerr effect (MOKE),[7–9] particularly in terms of its net transverse magnetization component M_T, which is perpendicular to the magnetic field.[9] Our initial MOKE measurements on Fe/FeF_2 gave evidence for coherent rotation only on the right side of the hysteresis loop, in contrast to the above PNR results. This called for systematic studies of the magnetization reversal asymmetry as to different directions of the in-plane cooling field with respect to the easy axis of the AFM and of the measurement-field variation about the cooling-field direction. This angular dependence is also aimed at investigating the role of higher-order anisotropies in asymmetric magnetization switching, especially of odd symmetry as considered previously.[10]

We present a systematic MOKE study of magnetization reversal in exchange-biased Fe/FeF_2 in terms of M_T, which may appear generally near the coercive fields.[9] Furthermore, this method allows us to determine the rotational *direction* (chirality) of the magnetization vector via the sign of M_T. Asymmetric magnetization reversal here is defined as appearance of a nonzero transverse magnetization component near only one coercive field of a hysteresis loop.

A totally unexpected behavior of M_T is found for different directions of the initial cooling field all over 360°, about which the measuring field is varied. For example, for the cooling field along the easy axis of the AFM FeF_2, the variation in the measuring field by only ±3° about this direction results in two asymmetric transverse loops of opposite signs. In these loops the M_T component vanishes on one or the other side of the hysteresis loop. These loops are simulated by a simple model describing the coherent rotation of a single magnetic moment or macrospin using a total energy density comprising generally noncollinear unidirectional and fourfold anisotropies. With the same set of parameters, the model reproduces also the "phase diagram" of characteristic M_T loops for cooling-field directions throughout 360°. We demonstrate that asymmetric magnetization reversal, originating from the unidirectional (EB) anisotropy, can be observed only along certain "phase lines" for which the measuring-field direction is noncollinear with both the cooling-field direction and the direction of the exchange bias. These field directions coincide throughout 360° only near the easy and the hard axes. We argue that only coherent rotation is sufficient in describing asymmetric magnetization reversal under these rather general anisotropy and angular measurement conditions.

Epitaxial, twinned $FeF_2(110)$ has been grown by molecular beam epitaxy on a MgO(100) single-crystal substrate. The complete multilayer structure MgO/FeF_2 (110 nm)/Fe (13 nm)/Al (10 nm) consisted additionally of polycrystalline Fe with (110) texture and an Al cap layer. Details of the sample preparation and structural characterization are given elsewhere.[11]

MOKE measurements have been carried out inside a magneto-optical cryostat with the external-magnetic-field direction aligned parallel to the film plane. A motorized sample rotator enabled sample rotations by about 360° with a precision of ±0.1°. For MOKE we chose a reflection plane parallel to the transverse magnetization component M_T of our sample and perpendicular to the external-magnetic-field di-

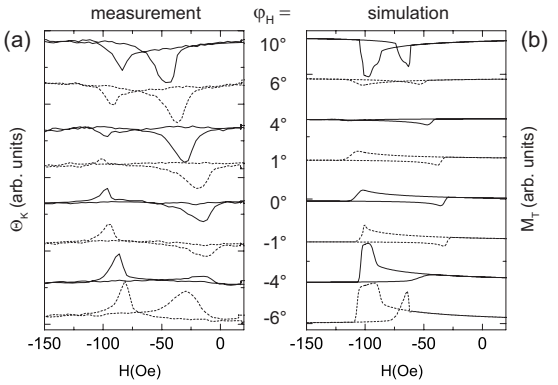

FIG. 1. (a) Transverse Kerr signal (Kerr rotation angle θ_K), which is proportional to M_T, as a function of magnetic field for $Fe/FeF_2(110)$ at $T=20$ K. The sample has been field cooled along the easy axis of the AFM layer ($\varphi_{FC}=0°$) in $H=1$ kOe. The magnetic field has been applied under different angles $\varphi_H>0$ ($\varphi_H<0$) by rotating the sample clockwise (counterclockwise). (b) Simulated M_T vs H hysteresis loops for different sample orientations using the simple model (see text).

rection. To unambiguously detect a pure M_T hysteresis loop, we chose incident light polarized perpendicular to the reflection plane (s polarized). Details of the experimental setup are described in Ref. 9.

We first investigate how the magnetization reversal depends on the measuring-field direction (φ_H), which we vary about the cooling-field direction ($\varphi_{FC}=0°$) along the easy axis of the antiferromagnetic FeF_2 layer (at 45° with respect to the AFM twins along the ⟨001⟩ directions). Figure 1(a) shows a series of transverse hysteresis loops taken at $T=20$ K for different sample orientations (positive angles correspond to a clockwise rotation of the sample). The data have been taken after field cooling at $\varphi_{FC}=0°$ in $H=1$ kOe. At $\varphi_H=-6°$ we clearly observe an M_T component near both coercive fields, indicating a symmetric reversal. Note that the sign of M_T is positive for both reversal directions, in contrast to the loop at, e.g., $\varphi_H=0°$ with opposite signs of M_T. A reversal similar to that at −6° is also seen at +6° but with the opposite sign of M_T. Most interestingly, M_T reverses asymmetrically, i.e., shows a vanishing M_T signal on only one side of the hysteresis loop between 1° and 4° (−1° and −4°) near the left (right) coercive field in Fig. 1(a) (see Fig. 3 for exact values). Note that these angles of sign change of M_T near *one* coercive field mark the field orientations of asymmetric magnetization reversal. On the other hand, at almost all field orientations we observe near the coercive fields a double-peaked M_T, which we attribute to coherent rotation of the magnetization vector. Two peaks of the same sign or alternating signs indicate coherent magnetization rotations in the same half plane or by 360°, such as in a Stoner-Wohlfarth model,[12] modified here by the relevant anisotropies. This suggests that coherent rotation of the magnetization may be the dominant reversal process at practically all stages of reversal.

To explain this scenario, we use a simple model describing the coherent rotation of a single magnetic moment or macrospin to simulate the prominent features of all M_T loops in Fig. 1(a). The reversal of the moment is induced by an external magnetic field under different angles $\varphi_H \neq 0°$ about the field cooling angle $\varphi_{FC}=0°$. For each field step the magnetic moment follows the minimum of a total energy density E comprising fourfold ($K^{(4)}$) and unidirectional ($K^{(1)}$) anisotropies. E is given by

$$E = -HM\cos(\varphi_M - \varphi_H) + K^{(4)}[\cos^2(\varphi_M - \varphi_4)\sin^2(\varphi_M - \varphi_4)] + K^{(1)}[\cos(\varphi_M - \varphi_{EB})],$$

where H describes the external magnetic field and M is the saturation magnetization of the FM layer; φ_H and φ_M are the angles of H and M, respectively, measured relative to the AFM easy axis. The angles φ_4 and φ_{EB} represent the corresponding angles of the fourfold and unidirectional easy axes, respectively. Note that the cooling-field angle φ_{FC} does not enter explicitly. For optimum values of the anisotropy constants, we obtained $K^{(1)}=-12.1\times10^3$ J/m^3 and $K^{(4)}=5.25\times10^3$ J/m^3 from the simulations of the transverse Kerr loops in Fig. 1(a). The angles result as $\varphi_4=5°$ and $\varphi_{EB}=3.5°$ for $\varphi_{FC}=0°$. These values were obtained by varying the parameters in the simulation in order to reproduce the measured coercive fields, exchange bias, and angles of vanishing M_T component on one side of the loop. The fourfold anisotropy constant $K^{(4)}$ of Fe is significantly smaller than single-crystal values in the literature.[13,14] This might be related to the polycrystalline fraction of the Fe film. For M we use the bulk value of 1760 Oe for iron.[14] The value of $K^{(1)}$ agrees within a factor of 3 with the one extracted from the literature.[10,15] Note that for $K^{(1)}=0$, we always obtain Stoner-Wohlfarth-type loops as for $\varphi_{FC}=\varphi_H=0°$.

In order to take into account changes in local anisotropies that might result from the polycrystalline structure of the Fe layer, we assume a small normal distribution of φ_4 and φ_{EB} with a standard deviation of $\sigma=0.5°$. These considerations enter mainly the line shapes in the simulations displayed in Fig. 1(b). Note that the *only* variable parameter is the direction of the external magnetic field φ_H. The sign change of M_T on one or the other side of the hysteresis loop proceeds in the simulation at the same angles as for the measured loops. Differences in the shape and position of the simulated and measured loops are attributed to the use of a simple macrospin model in the simulations, which neglects coupling between the magnetic moments and a resulting fanning. This is evident from more realistic Monte Carlo simulations by Beckmann *et al.*,[16,17] describing the magnetization reversal of an averaged ensemble of moments. Nevertheless, our simple macrospin model of coherent rotation can reproduce qualitatively all salient features of the magnetization reversal in the experiments. For example, for $-1° \leq \varphi_H \leq +1°$ the physics of the reversal mechanism in experiment and that in simulation are identical, despite slight differences in shape. From our simulation of the experimental data, we conclude that anisotropies of higher than fourth order and particularly of odd symmetry do not play a role in describing the reversal asymmetry in the EB system under investigation. This observation confirms the asymmetric reversal mode simulated by Beckmann *et al.* for untwinned[16] and twinned[17] EB systems.

In addition to the above experiments of varying φ_H about $\varphi_{FC}=0°$ along the AFM easy axis, we performed measure-

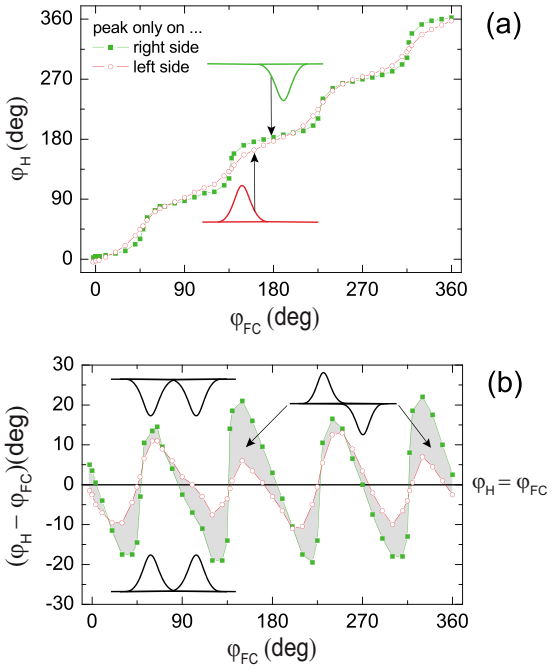

FIG. 2. (Color online) (a) Measuring-field angle φ_H at which for a given cooling-field angle φ_{FC} the transverse peak disappears asymmetrically on the left side (full green squares) or on the right side (open red circles) of the hysteresis loop; (b) phase diagram of $(\varphi_H - \varphi_{FC})$ as a function of the cooling-field direction φ_{FC}, with the phase lines from (a) separating the regimes of symmetrical and antisymmetrical reversal modes. The regimes are marked by the corresponding types of transverse magnetization loops.

ments at different cooling-field angles $\varphi_{FC} \neq 0°$ up to 360° about which we subsequently varied φ_H, in general with $\varphi_{FC} \neq \varphi_H$. The measurement-field angles φ_H at which M_T vanished on one or the other side of the loop are displayed in Fig. 2(a) as a function of φ_{FC}. Obviously for each cooling-field orientation there is a measurement-field angle (sample orientation) where M_T disappears on one side of the hysteresis loop. These phase lines principally follow the cooling-field angle but are superposed by a distinct fourfold "oscillation." In Fig. 2(b) we plot the difference between the measurement-field angle φ_H and cooling-field angle φ_{FC} as a function of the cooling-field direction. This results in the phase diagram with the phase lines as separations between symmetrical and antisymmetrical reversal modes. Here the fourfold symmetry is even more distinct. An additional twofold symmetry, weakly discernible by the maximum values of both phase lines, is not taken into account to keep the simulation as simple as possible.

The phase diagram can be understood as follows: For each cooling-field angle, measuring at a field angle located above the highest phase line (below the lowest phase line) will exhibit an M_T component with two peaks "down" ("up") on both sides of the loop. For angles in between the two phase lines, the two transverse peaks show different signs. This situation corresponds to a 360° Stoner-Wohlfarth-type rotation, modified here by the relevant anisotropies.

Beyond the above described simulation for $\varphi_{FC}=0°$ in Fig. 1(b), we now attempt to reproduce with the same set of

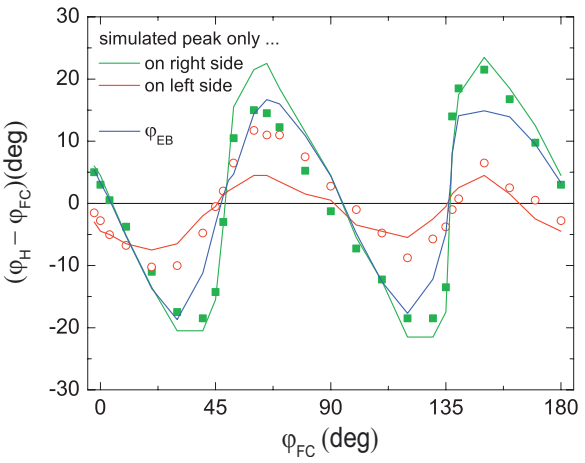

FIG. 3. (Color) Measured phase lines (full green squares and open red circles, averaged for better statistics over the two 180° intervals), determined exchange-bias angle φ_{EB} (blue line), and resultant simulated phase lines (green and red lines). AFM easy axes are located near 0° modulo 90°.

parameters the complete phase diagram in Fig. 2. One question arises as to the identification of the unidirectional (EB) easy axis (angle φ_{EB}) for different cooling-field directions (angle φ_{FC}). Parametrized simulations with different angles φ_{EB} show that for the measurement-field angle $\varphi_H = \varphi_{EB}$, the calculated M_T component exhibits always two peaks of opposite signs. This Stoner-Wohlfarth-type rotation (in between the phase lines) in most cases does not include the cooling-field direction [$\varphi_H = \varphi_{FC}$ in Fig. 2(b)]. Hence, the latter cannot in most cases be equal to the easy axis of the unidirectional anisotropy.

In order to determine the EB direction for general cooling-field and measurement-field directions, we carried out a parametrized simulation of the phase lines for different values of φ_{EB}. Comparison between the simulated phase lines as function of φ_{EB} and the measured phase lines as function of φ_{FC} yields a correlation between φ_{EB} and φ_{FC}. This is represented by the blue line in Fig. 3. The excursion of φ_{EB} from the experimentally set values of φ_{FC} is due to the anisotropies.

Under this assumption, the simulated phase lines (green/red lines in Fig. 3) describe the measured phase lines (full green squares and open red circles) fairly well. Larger deviations appearing in the phase diagram between the experimental data and the simulation for cooling-field angles between about 45° and 90° can be attributed to the neglect of the small twofold anisotropy.

Despite these deviations, our simple model with the same set of parameters is capable of reproducing in first order the magnetization reversal for cooling-field directions throughout 360°. It is obvious from Fig. 3 that the asymmetric magnetization reversal (phase lines) occurs for cooling-field angles all over 360° modulo 180°, for measuring fields which in general do not coincide with φ_{FC} and φ_{EB}. All these fields coincide throughout 360° only near roughly 0° modulo 45°, i.e., near the easy and hard axes.

A recently published paper dealing with asymmetric magnetization reversal in polycrystalline Co/IrMn relates the

asymmetry of the transverse magnetization component to the ratio of uniaxial FM anisotropy and unidirectional EB anisotropy as well as to the appearance of finite coercivity.[18] However, the authors treated only the special case of collinear uniaxial and unidirectional anisotropies and did not observe the appearance of a transverse magnetization component only on the right side of the hysteresis loop. Moreover, they did not vary the cooling-field direction and thus did neither cover nor predict the complexity of the different phases revealed in our work.

In summary, the magnetization reversal in exchange-biased $Fe/FeF_2(110)$ as probed by the transverse magnetization component M_T exhibits a complex phase diagram of different reversal modes. The phases depend strongly on the measuring-field angle φ_H and the cooling-field angle φ_{FC}, which is varied about 360°. Only the phase lines mark the actual locations of truly asymmetric magnetization reversal. The exchange-bias direction (angle φ_{EB}) is determined besides the cooling-field direction by the fourfold and unidirectional anisotropies. φ_{EB} coincides throughout 360° with φ_{FC} and φ_H only near the easy and hard axes. A simulation based on the coherent rotation of a macrospin considering generally noncollinear unidirectional and fourfold anisotropies can qualitatively describe the different reversal modes or "phases" of M_T. The agreement between simulation and experiment endorses the assumption that the phase lines of magnetization reversal in Fe/FeF_2, separating symmetrical and antisymmetrical reversal modes, can be deduced by a coherent rotation model.

We thank P. A. Crowell for providing the simulation code and we acknowledge useful discussions with U. Nowak. This work was supported by DFG through SPP1133/Be 2441/2-2, the U.S. DOE, and A. von Humboldt Foundation (I.K.S. and J.E.). One of us (I.K.S.) thanks the RWTH faculty and researchers for their hospitality during a sabbatical stay in Aachen.

*Present address: FTB, Hochschule Niederrhein, 41065 Mönchengladbach, Germany.
†Present address: IBI, Forschungszentrum Jülich, 52425 Jülich, Germany.
‡Corresponding author; gernot.guentherodt@physik.rwth-aachen.de
§Present address: Abteilung Festkörperphysik, Universität Ulm, 89069 Ulm, Germany.

[1] W. H. Meiklejohn and C. P. Bean, Phys. Rev. **105**, 904 (1957).
[2] For a review, see J. Nogués and I. K. Schuller, J. Magn. Magn. Mater. **192**, 203 (1999).
[3] For a review, see A. E. Berkowitz and K. Takano, J. Magn. Magn. Mater. **200**, 552 (1999).
[4] C. Leighton, M. R. Fitzsimmons, P. Yashar, A. Hoffmann, J. Nogués, J. Dura, C. F. Majkrzak, and Ivan K. Schuller, Phys. Rev. Lett. **86**, 4394 (2001).
[5] M. R. Fitzsimmons, P. Yashar, C. Leighton, Ivan K. Schuller, J. Nogués, C. F. Majkrzak, and J. A. Dura, Phys. Rev. Lett. **84**, 3986 (2000).
[6] F. Radu, M. Etzkorn, R. Siebrecht, T. Schmitte, K. Westerholt, and H. Zabel, Phys. Rev. B **67**, 134409 (2003).
[7] T. Mewes, H. Nembach, M. Rickart, S. O. Demokritov, J. Fassbender, and B. Hillebrands, Phys. Rev. B **65**, 224423 (2002).
[8] J. McCord, R. Schäfer, R. Mattheis, and K.-U. Barholz, J. Appl. Phys. **93**, 5491 (2003).
[9] A. Tillmanns, S. Oertker, B. Beschoten, G. Güntherodt, C. Leighton, Ivan K. Schuller, and J. Nogués, Appl. Phys. Lett. **89**, 202512 (2006).
[10] I. N. Krivorotov, C. Leighton, J. Nogués, Ivan K. Schuller, and E. D. Dahlberg, Phys. Rev. B **65**, 100402(R) (2002).
[11] J. Nogués, T. J. Moran, D. Lederman, Ivan K. Schuller, and K. V. Rao, Phys. Rev. B **59**, 6984 (1999).
[12] E. C. Stoner and E. P. Wohlfarth, Philos. Trans. R. Soc. London, Ser. A **240**, 599 (1948).
[13] U. Gradmann, in *Ferromagnetic Materials*, edited by K. H. J. Buschow (North-Holland, Amsterdam, 1993), Vol. 7, p. 1.
[14] E. P. Wohlfahrth, in *Ferromagnetic Materials*, edited by E. P. Wohlfahrth (North-Holland, Amsterdam, 1980), Vol. 1, p. 1.
[15] M. S. Lund, W. A. A. Macedo, Kai Liu, J. Nogués, Ivan K. Schuller, and C. Leighton, Phys. Rev. B **66**, 054422 (2002).
[16] B. Beckmann, U. Nowak, and K. D. Usadel, Phys. Rev. Lett. **91**, 187201 (2003).
[17] B. Beckmann, K. D. Usadel, and U. Nowak, Phys. Rev. B **74**, 054431 (2006).
[18] J. Camarero, J. Sort, A. Hoffmann, J. M. García-Martín, B. Dieny, R. Miranda, and J. Nogués, Phys. Rev. Lett. **95**, 057204 (2005).